

## Electronic Supplementary Information for

# Dipole Moments and Solvatochromism of Metal Complexes: Principle Photophysical and Theoretical Approach

Galina V. Loukova<sup>a\*</sup>, Alexey A. Milov<sup>b</sup>, Vladimir P. Vasiliev<sup>a</sup>,  
and Vladimir I. Minkin<sup>b,c</sup>

<sup>a</sup> *Institute of Problems of Chemical Physics, Russian Academy of Sciences,  
Acad. Semenov Ave., 1, Chernogolovka, Moscow Region, 142432 Russian Federation*

<sup>b</sup> *Southern Scientific Center, Russian Academy of Sciences,  
Chekhov Ave., 41, Rostov-on-Don, 344006, Russian Federation*

<sup>c</sup> *Southern Federal University, Institute of Physical and Organic Chemistry,  
Stachki Ave., 194/2, Rostov-on-Don, 344090, Russian Federation*

<b>Contents</b>	<b>pages</b>
Experimental Section	2
Table S1. Spectroscopic properties of <i>rac</i> -C <sub>6</sub> H <sub>10</sub> (IndH <sub>4</sub> ) <sub>2</sub> ZrCl <sub>2</sub> in 25 typical organics and the solvent polarity parameters	3
Solvatochromic Determination of Electric Dipole Moments	
Mathematical Treatment	4
Figure S1. Molecular structure of <i>rac</i> -C <sub>6</sub> H <sub>10</sub> (IndH <sub>4</sub> ) <sub>2</sub> ZrCl <sub>2</sub> with direction of $\mu$	6
Figure S2. Dependences of the Stokes shift on the solvent polarity parameters	7–8
Figure S3. The McRae-type dependences for <i>rac</i> -C <sub>6</sub> H <sub>10</sub> (IndH <sub>4</sub> ) <sub>2</sub> ZrCl <sub>2</sub> , Cp <sub>2</sub> ZrCl <sub>2</sub>	9
Table S2. Simulated dipole moments of Cp <sub>2</sub> ZrCl <sub>2</sub> in gas and 28 solvents	10
Figure S4. Absorption and emission spectra of Cp <sub>2</sub> ZrCl <sub>2</sub> in dichloroethane	11
Table S3. Absorption maxima of Cp <sub>2</sub> ZrCl <sub>2</sub> in solvents	11
Figure S5. Dependence of $\Delta\mu$ of the zirconocenes on solvent parameters	12
Computational Details	13
ESI References	14

---

\* Corresponding author.

E-mail: [gloukova@mail.ru](mailto:gloukova@mail.ru)

## Experimental Section

The zirconocenes, as other group 4 organometallic complexes, are air and moisture sensitive. Presently, all manipulations with zirconocene samples were performed under condition of rigorous exclusion of oxygen and moisture in flamed Schlenk-type glassware on a dual-manifold Schlenk line or interfaced to a high-vacuum line. The choice of organic solvents was motivated by three basic reasons: (i) solvents with differing bulk parameters  $\epsilon$  and  $n$  should be employed (ii) organic media typical for catalysis, organometallic and organic synthesis are of special interest (iii) zirconocenes are usually stable in aprotic organic solvents, treated rigorously with drying agents. The solvents were obtained from Fluka-Aldrich, Acros Organics, and Lancaster with purity of 99+%. The solvents (spectrophotometric grade, where possible) were additionally purified, rigorously dried by reflux over suitable drying agents ( $\text{LiAlH}_4$  or  $\text{CaH}_2$  and  $\text{P}_4\text{O}_{10}$ ) followed by distillation and degassed through several freeze-pump-thaw cycles. Purity of the solvents used was checked by monitoring UV-vis absorption and luminescence at 77 K and RT. For a proper comparison, the solvents were also treated with appropriate chemical agents in order to remove accidental traces of impurities and moisture. Afterwards, all photophysical data for the same solvents obtained from different commercial sources were collected and compared: very similar luminescence characteristics were obtained for the target zirconocene solutions under this condition.

Absorption spectra were measured on a UV-vis-NIR scanning spectrophotometer UV-3101PC (“Shimadzu Corporation”). Steady-state emission spectra were recorded with a Perkin-Elmer LS-55 spectrofluorimeter the spectra were recorded upon excitation of the sample solutions: at  $\lambda_{\text{exc}} = 350\text{--}360$  nm [*rac*- $\text{C}_6\text{H}_{10}(\text{IndH}_4)_2\text{ZrCl}_2$  (**1**)] and 325–335 nm [ $\text{Cp}_2\text{ZrCl}_2$  (**2**)]. The luminescence spectra do not change with the change in the excitation light wavelength. The sample solutions, obtained with use of single crystals. Sample solutions were kept dilute ( $10^{-5}$ – $10^{-4}$  M) in order to prevent concentration effects. Measurements were performed in 1-cm optical quartz cells at 20 °C.

*The polarities of the solvents* (Table S1) are estimated using the definition of the Bakhshiev

solvent polarity parameter  $F_{\text{B}}(\epsilon, n^2)$ , viz.:  $F_{\text{B}} = \frac{2n^2 + 1}{n^2 + 2} \left( \frac{\epsilon - 1}{\epsilon + 2} - \frac{n^2 - 1}{n^2 + 2} \right)$ , and the Bilot-Kawski

solvent polarity parameter  $F_{\text{B-K}}(\epsilon, n^2)$ , viz.:  $F_{\text{B-K}} = \frac{2n^2 + 1}{n^2 + 2} \left( \frac{\epsilon - 1}{\epsilon + 2} - \frac{n^2 - 1}{n^2 + 2} \right) + 2 \frac{3}{2} \frac{n^4 - 1}{(n^2 + 2)^2}$ .

The McRae solvent polarity parameter is  $F_{\text{MR}}(\epsilon, n^2)$ , viz.:  $F_{\text{MR}} = \left( \frac{\epsilon - 1}{\epsilon + 2} - \frac{n^2 - 1}{n^2 + 2} \right)$ , where “optic

dielectric constant”,  $n^2$ , is the square of the refractive index and  $\epsilon$  is the dielectric permittivity of the solvent. Dielectric constants ( $\epsilon$ ) and refractive indices ( $n$ ) of neat solvents were obtained from available literature.

**Table S1** R.T. Spectroscopic Properties of **1** in 25 Typical Organics and the Solvent Polarity Parameters

Solvents	$\epsilon$	$n$	$F_B^a$	$F_{B-K}^b$	$F_{MR}^c$	$\nu_A, \text{cm}^{-1}$	$\nu_E, \text{cm}^{-1}$	$\Delta\nu, \text{cm}^{-1}$
1,2-dichloroethane	10.36	1.4450	0.62185	1.22498	0.49113	27550	21050	6500
dichloromethane	9.080	1.4240	0.59504	1.1705	0.47407	27550	20950	6600
trichloromethane	4.806	1.4460	0.37056	0.97501	0.29254	27620	21100	6520
tetrachloromethane	2.240	1.4595	0.02397	0.64611	0.01882	28250	21900	6350
benzene	2.280	1.5010	0.00576	0.68179	0.00445	28000	21800	6200
toluene	2.380	1.4960	0.02965	0.69923	0.02295	28050	21900	6150
ethylbenzene	2.410	1.4959	0.03573	0.70518	0.02766	28000	22000	6000
<i>iso</i> -propylbenzene	2.380	1.4910	0.03282	0.69594	0.02545	28050	22000	6050
<i>sec</i> -butylbenzene	2.320	1.4890	0.02183	0.68236	0.01694	28050	22000	6050
1,2-xylene	2.568	1.5050	0.06049	0.74167	0.04665	28000	22000	6000
1,3-xylene	2.374	1.4790	0.03922	0.68678	0.03056	28000	22000	6000
1,4-xylene	2.270	1.4950	0.00749	0.67578	0.0058	28000	22000	6000
1,2-dichlorobenzene	9.930	1.5510	0.56651	1.3064	0.42948	27700	21500	6200
chlorobenzene	5.620	1.5240	0.39222	1.09778	0.30033	27700	21600	6100
1,4-chlorotoluene	6.100	1.5200	0.42461	1.12505	0.32562	27700	21550	6150
hexene-1	2.100	1.3880	0.03995	0.56757	0.03232	28500	22450	6050
<i>n</i> -pentane	1.840	1.3570	0	0.48571	0	28500	22650	5850
<i>n</i> -hexane	1.880	1.3750	0	0.50764	0	28500	22650	5850
cyclohexane	2.023	1.4250	0	0.57501	0	28500	22650	5850
methylcyclohexane	2.020	1.4231	0	0.57305	0	28500	22650	5850
tetrahydrofuran	7.580	1.4070	0.54916	1.10209	0.44068	28000	21900	6100
2-methyltetrahydrofuran	6.970	1.4060	0.52307	1.07467	0.41992	28100	21900	6200
2,5-dimethyltetrahydrofuran	6.160	1.4040	0.48263	1.03157	0.38779	28100	21900	6200
<i>tert</i> -butylmethyl ether	4.500	1.3690	0.38341	0.8856	0.31282	28150	21950	6200
acetonitrile	37.50	1.3390	0.86447	1.32628	0.715	27500	20800	6700

Notes: Dielectric characteristics  $\epsilon$  and  $n$  of the solvents were taken from standard sources.

<sup>a</sup>  $F_B(\epsilon, n^2)$  stands for the Bakhshiev solvent polarity parameter.

<sup>b</sup>  $F_{B-K}(\epsilon, n^2)$  stands for the Bilot-Kawski solvent polarity parameter.

<sup>c</sup>  $F_{MR}(\epsilon, n^2)$  stands for the McRae solvent polarity parameter.

$\nu_A$  is the maximum of the lowest-energy absorption band (corresponds to the electronic transition between FMOs: LMCT).  $\nu_E$  is the emission maximum.  $\Delta\nu$  is the Stokes shift.

We note on passing that absorption and emission spectra of **1** are similar for the groups of closely related solvents: alkanes, aromatic hydrocarbons (benzene, toluene, xylenes, etc.), ethers (THF, 2-MeTHF, 2,5-Me<sub>2</sub>THF, <sup>t</sup>BuOMe), and so on.

## Solvatochromic Determination of Electric Dipole Moments:

### Mathematical Treatment

Most theoretical treatments of solvatochromism are based on a solvent dielectric field model, where the dipole of a polar solute polarizes the surrounding solvent molecules, in turn, producing an electric field that perturbs the energy levels of the solute. Although complete equations to describe solvatochromic shifts are quite sophisticated and do not treat specific interactions (such as donor – acceptor coordination, H-bonding, etc.), more or less simplified forms have been successfully applied to treat organic systems. The difference in the known solvatochromic studies on organic solutes is referred to different solvent dielectric functions applied. It was thought that different dielectric functions would cover different classes of organic solutes. Meanwhile, most theories unraveling solvent effects on the location of absorption and emission spectra, in spite of different assumptions, suggest quite similar expressions for Stokes shift.

The employment of simple quantum-mechanical second-order perturbation method and consideration of the Onsager model of reaction field for a polarizable dipole, resulted in the two principle equations for the difference and sum of absorption ( $\nu_A$ ) and emission ( $\nu_E$ ) maxima wavenumbers:

1) Bakhshiev equation [1]:

$$\nu_A - \nu_E = \Delta\nu = m_1 F_B(\varepsilon, n^2) + \text{constant} \quad (1)$$

2) Bilot-Kawski equation [2-4]:

$$\nu_A + \nu_E = -m_2 F_{B-K}(\varepsilon, n^2) + \text{constant} \quad (2)$$

where  $F_{B-K}(\varepsilon, n^2)$  is the sum  $F_B(\varepsilon, n^2) + 2g(n^2)$ .

$$m_1 = \frac{2(\mu_e - \mu_g)^2}{hca^3} \quad (3)$$

$$m_2 = \frac{2(\mu_e^2 - \mu_g^2)}{hca^3} \quad (4)$$

where  $h$  is the Planck's constant,  $c$  is velocity of light,  $a$  is the solvent cavity radius (for **1**: assumed to be 5.65 Å, according to our B3LYP/QZVP calculations), and the bulk dielectric properties of solvents:  $\varepsilon$  denotes the electric permittivity and  $n$  is the refractive index. Respectively, the parameters  $m_1$  and  $m_2$  can be derived from the absorption and emission band shifts linear regressions (1) and (2) as the slopes. [2]

Below is a scheme simplifying to some extent the solvent polarity parameters. Thus, assuming a spherical cavity with an Onsager radius  $a$ , the key polarity parameters become:

$$F_B(\varepsilon, n^2) = \frac{\frac{\varepsilon-1}{2\varepsilon+1} - \frac{n^2-1}{2n^2+1}}{\left(1 - \frac{2\alpha}{a^3} \frac{\varepsilon-1}{2\varepsilon+1}\right) \left(1 - \frac{2\alpha}{a^3} \frac{n^2-1}{2n^2+1}\right)^2} \quad (5)$$

$$g(n^2) = \frac{\frac{n^2-1}{2n^2+1} \left(1 - \frac{\alpha}{a^3} \frac{n^2-1}{2n^2+1}\right)}{\left(1 - \frac{2\alpha}{a^3} \frac{n^2-1}{2n^2+1}\right)^2} \quad (6)$$

If the polarizability  $\alpha$  of the solute can be neglected ( $\alpha \sim 0$ ), the equation for  $F_{L-M}(\varepsilon, n^2) = \left(\frac{\varepsilon-1}{2\varepsilon+1} - \frac{n^2-1}{2n^2+1}\right)$  obtained by Lippert [5] and Mataga et al. [6] results from Eq. (5). For an isotropic polarizability of the solute, the condition  $2\alpha/a^3 = 1$  is frequently satisfied and relations (5) and (6) are thus simplified:

$$F_B(\varepsilon, n^2) = \frac{2n^2+1}{n^2+2} \left( \frac{\varepsilon-1}{\varepsilon+2} - \frac{n^2-1}{n^2+2} \right) \quad (7)$$

$$\text{and } g(n^2) = \frac{3}{2} \frac{n^4-1}{(n^2+2)^2} \quad (8)$$

Assuming that the solute symmetry remains unchanged upon electronic transition and the ground- and excited-state dipole moments are parallel (*this is, indeed, our case*: Fig. 1) and with the use of (3) and (4), the following expressions can be obtained [3, 7-8]:

$$\mu_g = \frac{1}{2}(m_2 - m_1) \left(\frac{1}{2} hca^3 / m_1\right)^{1/2} \quad (9)$$

$$\mu_e = \frac{1}{2}(m_1 + m_2) \left(\frac{1}{2} hca^3 / m_1\right)^{1/2} \quad (10)$$

$$\mu_e = \mu_g \frac{m_1 + m_2}{m_2 - m_1}, (m_1 < m_2) \quad (11)$$

The theoretical basis is only outlined here details of the mathematical treatment are given in the above cited references. In addition, let us note that, in general, the dipole moments  $\mu_g$  and  $\mu_e$  are not necessarily parallel but form some angle  $\varphi$ .

Dipole moment is a measure of the molecular charge distribution, a 3D vector, and can be applied as a descriptor to depict the charge movement across the molecule. Directions of the molecular dipole moment vector are dependent on the positions (centers) of the positive and negative charge. Notably, the parallelism between the ground and excited-state dipole moments

(Fig. S1) reveals the larger charge movement across **1** in the excited-state than that in the ground state in the same direction.

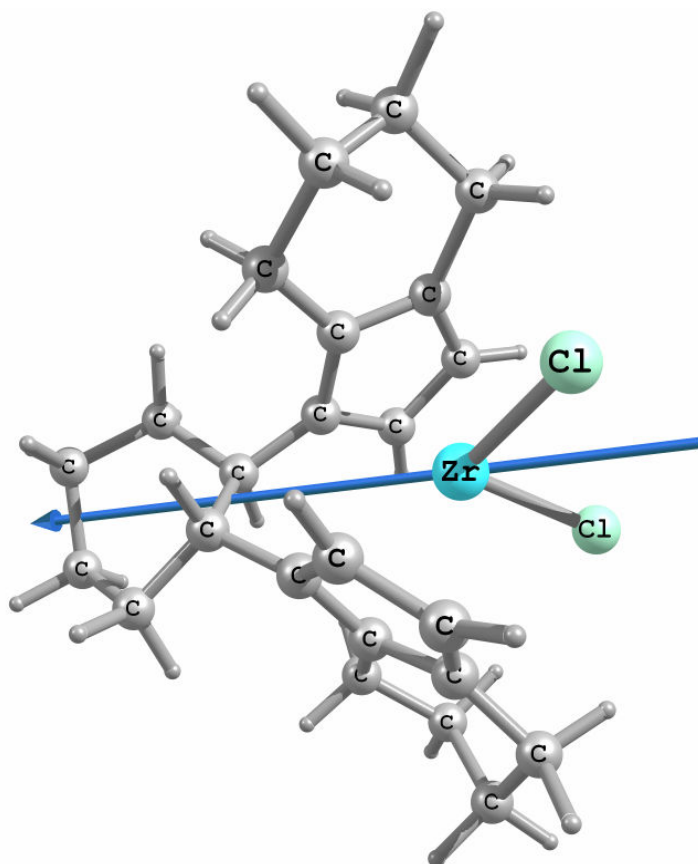
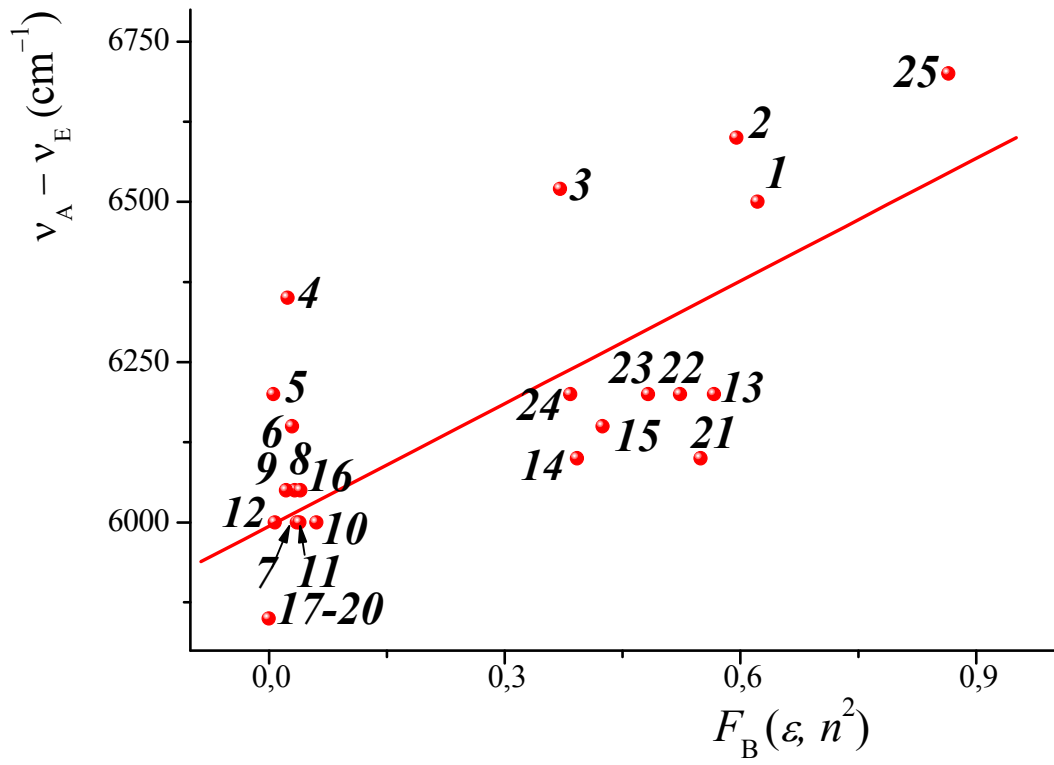
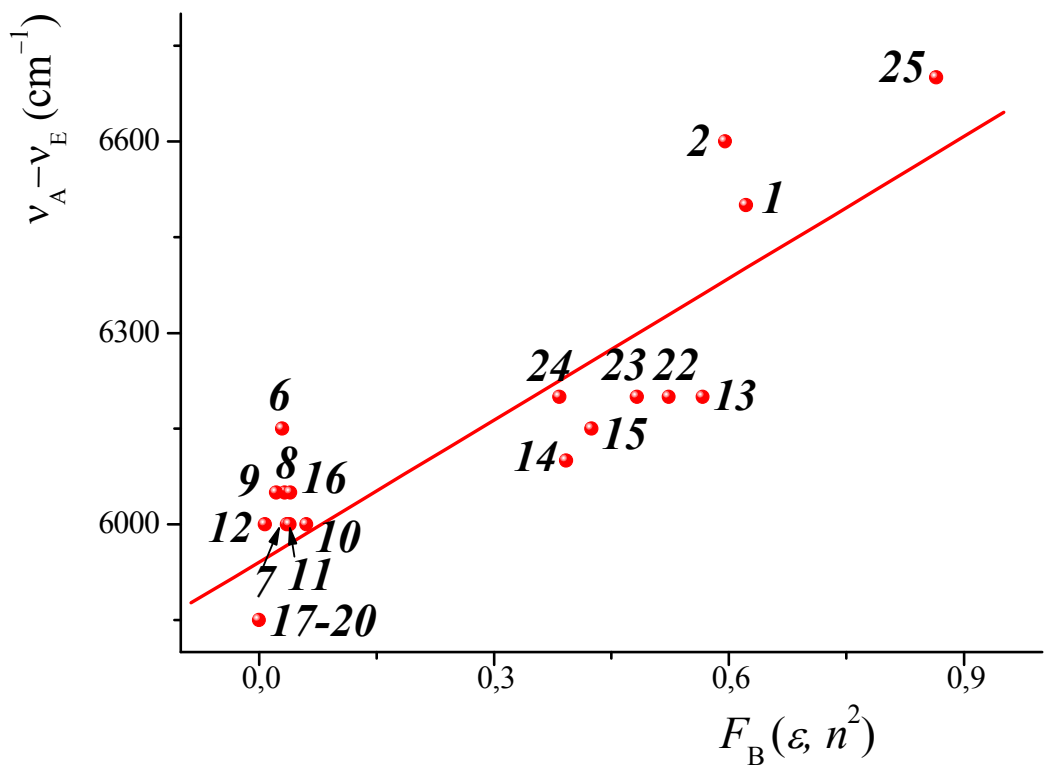


**Fig. S1** Molecular structure of **1** demonstrating direction of the electric dipole moment both in the ground and excited states ( $\vec{\mu}_g \parallel \vec{\mu}_e$ ). Simulation at the DFT/B3LYP/QZVP level of theory.

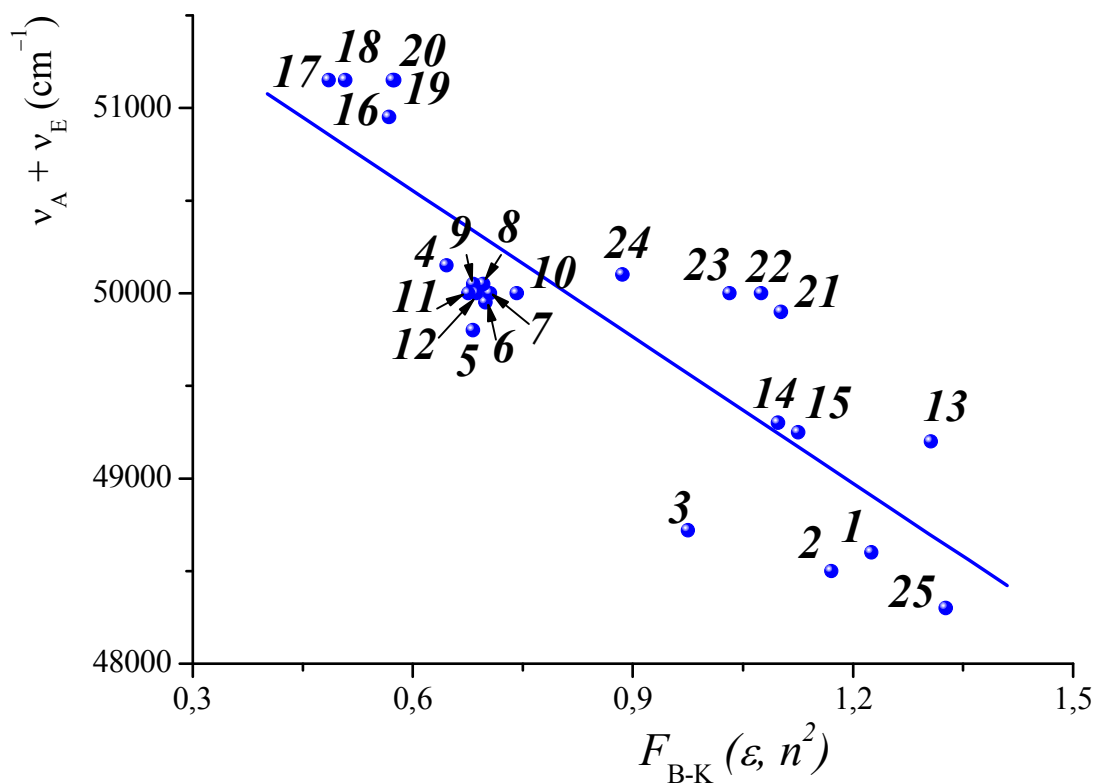
Figures S2 *a–c* demonstrate the dependences of the Stokes shift of dissolved **1** on the Bakhshiev and Bilot-Kawski solvent polarity parameters and the respective numerical solutions. A few solvents generate results that deviate from the least-squares fitting and correspond to non-polar or low-polar media and hence may not be included in  $\mu$  determination. Respectively, data points 3–5 and 21, corresponding to non-polar or rather low polar solvents ( $\text{CHCl}_3$ ,  $\text{CCl}_4$ ,  $\text{C}_6\text{H}_6$ , and THF), can be removed, see: Fig. S2 *b*).



(a)



(b)



(c)

**Fig. S2** The dependences of the Stokes shift of dissolved **1** on the **Bakhshiev** solvent polarity parameter  $F_B(\varepsilon, n^2)$  (a, b). The dependence of the sum of energies of the HOMO–LUMO absorption and emission maxima of dissolved **1** on the **Bilot-Kawski** solvent polarity parameter  $F_{B-K}(\varepsilon, n^2)$  (c). The 25 common organic solvents appear in the order: 1,2- $C_2H_4Cl_2$  (1),  $CH_2Cl_2$  (2),  $CHCl_3$  (3),  $CCl_4$  (4),  $C_6H_6$  (5), toluene (6), ethylbenzene (7), *i*-propylbenzene (8), *sec*-butylbenzene (9), *o*-, *m*-, *p*-xylene (10, 11, 12), 1,2- $C_6H_4Cl_2$  (13),  $C_6H_5Cl$  (14), 1,4-chlorotoluene (15), hexene-1 (16),  $n$ - $C_5H_{12}$  (17),  $n$ - $C_6H_{14}$  (18), cyclohexane (19), methylcyclohexane (20), THF (21), 2-MeTHF (22), 2,5-Me<sub>2</sub>THF (23), *t*BuOMe (24), MeCN (25).

The least-squares lines represent the best fit of the data points to the **Bakhshiev** relationship:  $\nu_A - \nu_E = \Delta\nu = 6.0 \times 10^3 + 0.64 \times 10^3 F_B$  (all points data,  $r^2 = 0.74$ ) (a) and  $\nu_A - \nu_E = \Delta\nu = 6.0 \times 10^3 + 0.74 \times 10^3 F_B$  (21 selected points data,  $r^2 = 0.88$ ) (b), the **Bilot-Kawski** relationship:  $\nu_A + \nu_E = 5.2 \times 10^4 - 2.6 \times 10^3 F_{B-K}$  ( $r^2 = 0.85$ ) (c).

$$3) \text{ McRae equation [9]: } \Delta\nu_A = (AL_0 + B) \frac{n^2 - 1}{2n^2 + 1} + C \left( \frac{\varepsilon - 1}{\varepsilon + 2} - \frac{n^2 - 1}{n^2 + 2} \right) \quad (12)$$

$A$ ,  $B$ , and  $C$  are the constants being characteristic of the solute,

$$\text{where } C = \frac{2}{hca^3} (\mu_g - \mu_e) \mu_g \quad (13)$$

and  $\Delta\nu_A = \nu_{A(\text{solv})} - \nu_{A(\text{gas})}$  is the difference between the energy of the optical transition in the solvent and in the gas phase. The coefficient  $C$  can be obtained from a least-squares fit of the absorption wavenumbers  $\nu_A$  ( $\text{cm}^{-1}$ ) of the target solute in solvents against the McRae solvent

polarity parameter  $F_{\text{MR}} = \left( \frac{\varepsilon - 1}{\varepsilon + 2} - \frac{n^2 - 1}{n^2 + 2} \right)$  (Fig. S3).

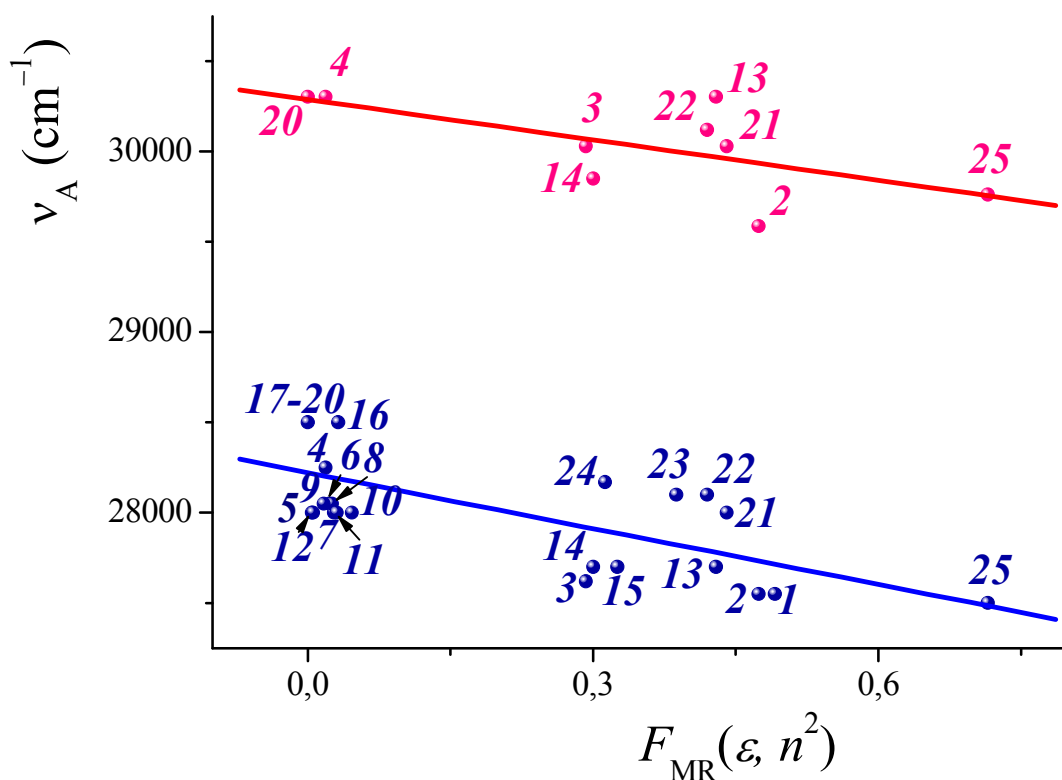


**Fig. S3** The dependences of the absorption maxima energies on the McRae solvent polarity parameter  $F_{\text{MR}}$ . The 25 common organic solvents appear in the order: 1,2- $\text{C}_2\text{H}_4\text{Cl}_2$  (1),  $\text{CH}_2\text{Cl}_2$  (2),  $\text{CHCl}_3$  (3),  $\text{CCl}_4$  (4),  $\text{C}_6\text{H}_6$  (5), toluene (6), ethylbenzene (7), *i*-propylbenzene (8), *sec*-butylbenzene (9), *o*-, *m*-, *p*-xylene (10, 11, 12), 1,2- $\text{C}_6\text{H}_4\text{Cl}_2$  (13),  $\text{C}_6\text{H}_5\text{Cl}$  (14), 1,4-chlorotoluene (15), hexene-1 (16), *n*- $\text{C}_5\text{H}_{12}$  (17), *n*- $\text{C}_6\text{H}_{14}$  (18), cyclohexane (19), methylcyclohexane (20), THF (21), 2-MeTHF (22), 2,5-Me<sub>2</sub>THF (23), *t*BuOMe (24), MeCN (25).

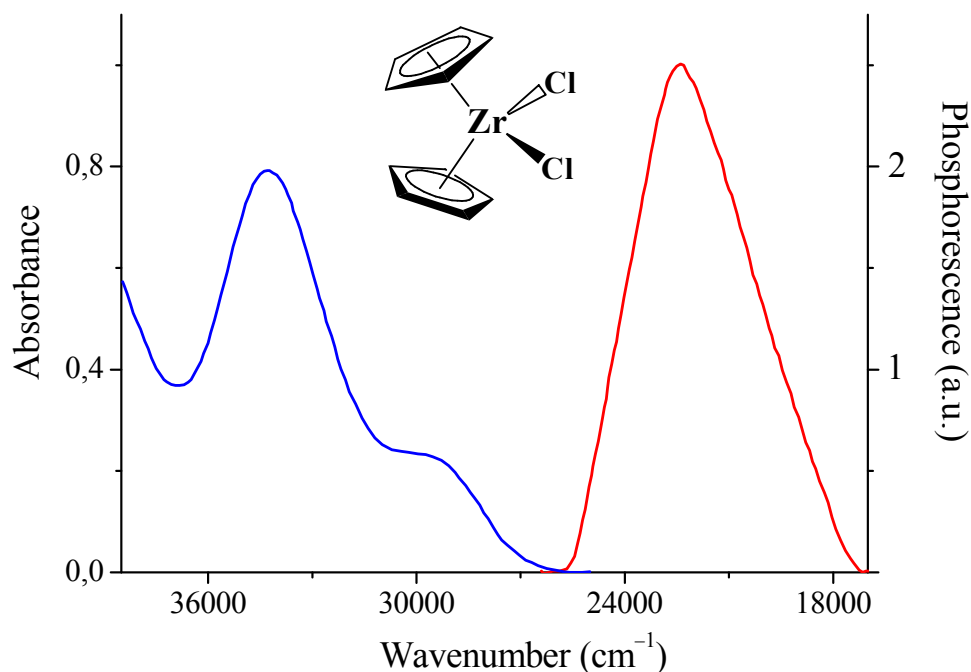
The least-squares lines represent best fit of the experimental data points to the McRae relationship: for **1** (blue colour),  $\nu_A = 2.8 \times 10^4 - 1.03 \times 10^3 F_{\text{MR}}$  ( $r^2 = 0.71$ ) and for **2** (red colour),  $\nu_A = 3.0 \times 10^4 - 0.74 \times 10^3 F_{\text{MR}}$  ( $r^2 = 0.65$ ).

The dipole moment of **1** in the ground state is minimal in gas phase (5.46 D), alkanes (6.4 D), and alkenes (6.5 D), while is maximal in the most polar solvent used, acetonitrile (8.85 D) i.e. the increase of  $\mu_g$  due to a polar medium is as large as 62 % (at hypothetical transfer from gas to MeCN) and 38% (at transfer from the non-polar solvents to MeCN). An analogous tendency is observed for the triplet-state dipole moment: the smallest  $\mu_e$  value is obtained for the gas phase (8.07 D), while the largest  $\mu_e$  value (13.66 D) is in acetonitrile. The increase of  $\mu_e$  on going from gas phase and non-polar solvents to acetonitrile is as large as 69 % and 39%, respectively. These data clearly suggest that a substantial excited-state dipole moment must exist for all cases. The same trend in the ground and excited-state dipole moments is observed in case of parent **2** (Table S2).

**Table S2** Electric dipole moments of  $\text{Cp}_2\text{ZrCl}_2$  in the ground and emissive  $^3\text{LMCT}$  state and their difference in gas phase and in the 28 typical organic media simulated at the B3LYP/QZVP level of theory.

Solvent	$\epsilon$	Dipole moment (Debye)		
		$\mu_g$	$\mu_e$	$\Delta\mu$
gas	1	4.60	6.62	2.02
benzene	2.28	5.71	8.82	3.11
toluene	2.38	5.77	8.89	3.12
ethylbenzene	2.41	5.79	8.95	3.16
1,2-xylene	2.568	5.84	9.07	3.23
1,3-xylene	2.374	5.76	8.85	3.09
1,4-xylene	2.27	5.72	8.78	3.06
chlorobenzene	5.62	6.74	10.53	3.79
1,2-dichlorobenzene	9.93	7.19	11.23	4.04
<i>n</i> -pentane	1.84	5.43	8.18	2.75
<i>n</i> -hexane	1.88	5.46	8.25	2.79
cyclohexane	2.023	5.56	8.41	2.85
methylcyclohexane	2.02	5.55	8.42	2.87
hexene-1	2.1	5.60	8.48	2.88
dichloromethane	10.36	7.11	11.10	3.99
tetrachloromethane	2.24	5.68	8.73	3.05
1,2-dichloroethane	10.36	7.19	11.24	4.05
trichloromethane	4.806	6.56	10.23	3.67
acetonitrile	37.5	7.73	12.19	4.46
tetrahydrofuran	7.58	6.97	10.96	3.99
diethyl ether	4.335	6.44	10.09	3.65
bromobenzene	5.40	6.70	10.45	3.75
fluorobenzene	5.42	6.70	10.45	3.75
<i>iso</i> -propylbenzene	2.38	5.78	8.89	3.11
1,3,5-trimethylbenzene	2.265	5.71	8.85	3.14
diisopropyl ether	3.38	6.19	9.67	3.48
<i>n</i> -butylbenzene	2.36	5.75	8.86	3.11
<i>sec</i> -butylbenzene	2.32	5.77	8.86	3.09
<i>tert</i> -butylbenzene	2.3447	5.77	8.85	3.08

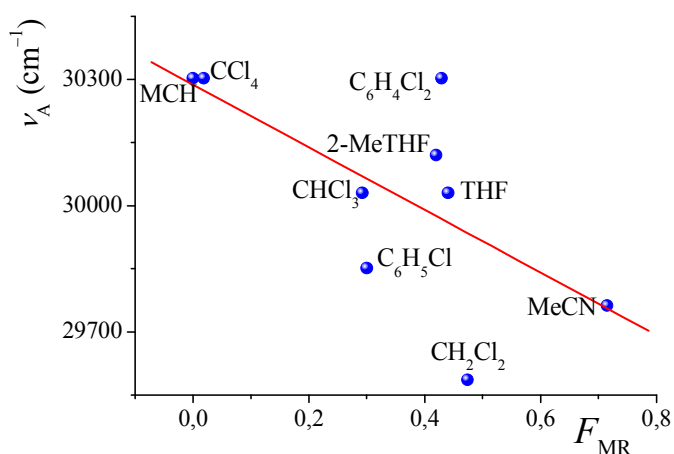
$\text{Cp}_2\text{ZrCl}_2$  possesses rather weak phosphorescence (e.g.  $\Phi_{\text{em}} \sim 0.01$  in dichloroethane) in room-temperature solutions (Fig. S4), while it is highly emissive in glassy solutions.



**Fig. S4** Absorption and emission ( $\lambda_{\text{exc}} = 330 \text{ nm}$ ) spectra of **2** in dichloroethane at room temperature.

**Table S3** The first LMCT absorption maxima of  $\text{Cp}_2\text{ZrCl}_2$  dissolved in the selected organic solvents and the dependence on the McRae solvent polarity parameter.

Solvent	$\lambda_A$ (nm)
methylcyclohexane (MCH)	330
tetrachloromethane	330
trichloromethane	333
chlorobenzene	335
2-methyltetrahydrofuran	332
tetrahydrofuran	333
1,2-dichlorobenzene	330
dichloromethane	338
acetonitrile	336



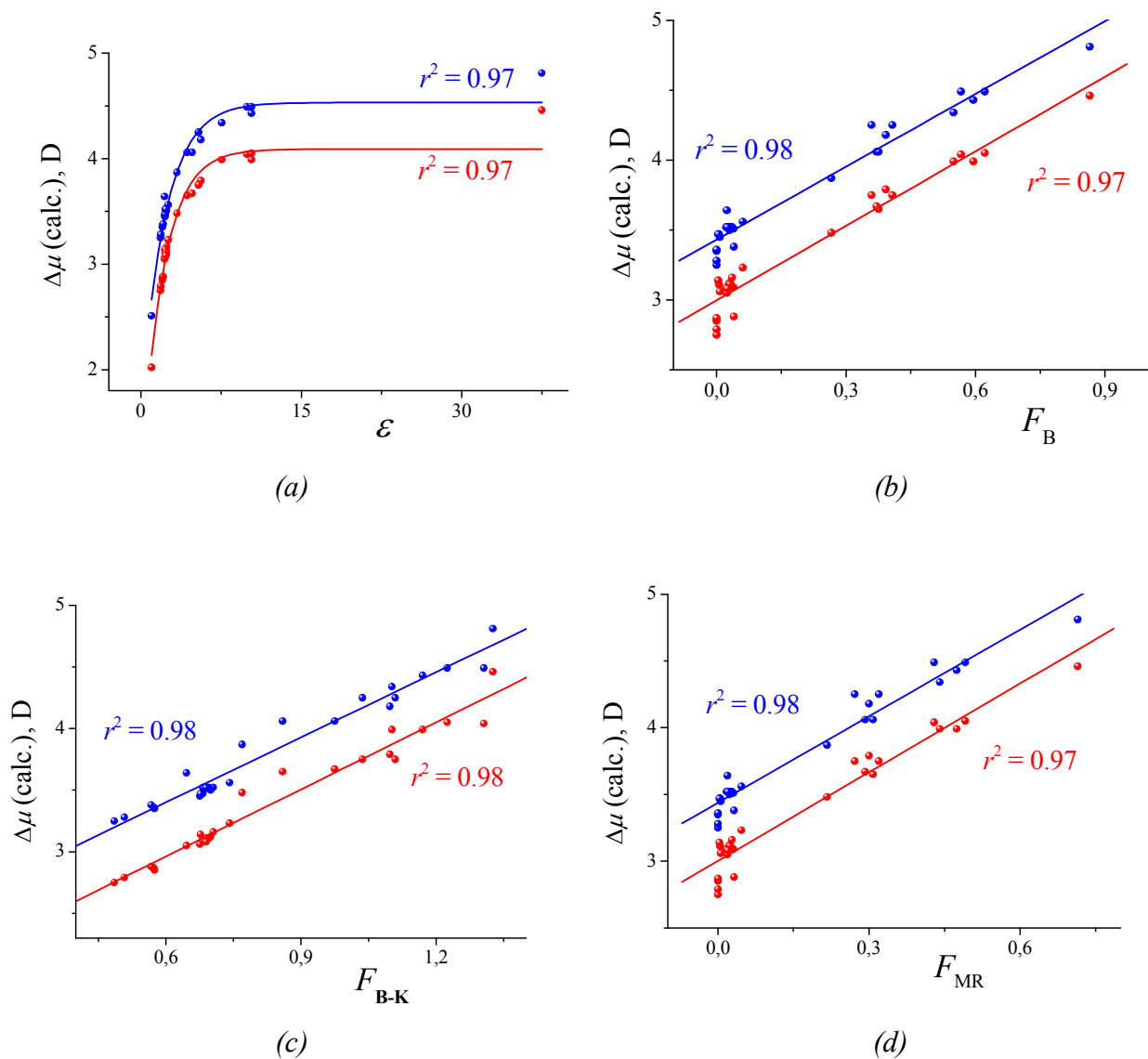


**Fig. S5** General patterns of evolution of theoretical values  $\Delta\mu$ , corresponding to **1 (blue colour)** and **2 (red colour)**, with the increase of solvent dielectric permittivity  $\varepsilon$  (a), Bakhshiev  $F_B(\varepsilon, n^2)$  (b), Bilot-Kawski  $F_{B-K}(\varepsilon, n^2)$  (c), and McRae  $F_{MR}(\varepsilon, n^2)$  (d) solvent polarity parameters.

As can be seen in Fig. S5 (b–d), all relationships  $\Delta\mu$  vs. solvent polarity functions were found to be linear with correlation coefficient equal or larger 0.97. The linearity of these dependences  $\Delta\mu$  (vs.  $F$ ) corresponds to the dominant importance of the general polarity effects on the theoretical values of  $\Delta\mu$  (as well as  $\mu_g$  and  $\mu_e$ ).

## Computational Details

In order to model the ground and excited-state properties of the zirconocenes in gas phase and in organic solvents, we applied density functional theory at the B3LYP/QZVP level the calculations were performed with use of the Gaussian 09 suite of programs. [10] On successive application of DFT methods to unraveling properties of complex organic molecules and transition metal complexes, see recent reviews, e.g.: [11–14]. Dipole moments of the studied organometallic compounds in  $S_0$  and  $T_1$  states were obtained using standard procedure of search for stationary points on different potential energy surfaces with different multiplicity (procedure “OPT FREQ” (geometry optimisation plus frequency analysis)) [15].

The methodology, we have used to include environment effects, is the polarizable continuum model (PCM). The PCM procedure [16–18], one of the most widely used continuum dielectric methods, is applied herein to estimate the solvent effects on electronic structures, especially on the electric dipole moments of **1**, **2** in the ground and phosphorescent electronic states. Our methodology captured the key features of the problem, such as an accurate calculation of electronic excited states, the shape of molecules, and the response of the surrounding medium to charge and, importantly, to transition densities. All results reported in the present work are obtained for the structures, corresponding to the minima on the potential energy surface. The Onsager radius  $a$  was computed it is worse noting that in the framework of the Gaussian 09 program, the molecular volume is defined as the volume inside a contour of 0.001 electron/Bohr<sup>3</sup> density and the output radius is 0.5 Å larger than the radius corresponding to the computed volume.

## ESI References

- (1) N. G. Bakhshiev, M. I. Knyazhanskii, V. I. Minkin, O. A. Osipov and G. V. Saidov, *Usp. Khim.*, 1969, **38:9**, 1644–1673 and references cited therein.
- (2) A. Kowski, *Z. Naturforsch.*, 2002, **57a**, 255–262.
- (3) A. Kowski, in: J. F. Rabek, Ed. *Prog. Photochem. Photophys.*, vol. 5, CRC Press, Boca Raton, Ann. Arbor, Boston, 1992, p. 1 (here a broad review of earlier literature is given).
- (4) L. Bilot and A. Kowski, *Z. Naturforsch.*, 1962, **17a**, 621–627.
- (5) E. Lippert, *Ber. Bunsenges. Phys. Chem.*, 1957, **61**, 962–975.
- (6) N. Mataga, Y. Kaifu and M. Kozumi, *Bull. Chem. Soc. Jpn.*, 1956, **29**, 465–470.
- (7) L. Bilot and A. Kowski, *Z. Naturforsch.*, 1963, **18a**, 256–256.
- (8) A. Kowski, *Naturwissenschaften*, 1964, **51**, 82–83.
- (9) E. G. McRae, *J. Phys. Chem.*, 1957, **61**, 562–572.
- (10) *Gaussian 09, Revision D.01*, M. J. Frisch, G. W. Trucks, H. B. Schlegel, G. E. Scuseria, M. A. Robb, J. R. Cheeseman, G. Scalmani, V. Barone, B. Mennucci, G. A. Petersson, H. Nakatsuji, M. Caricato, X. Li, H. P. Hratchian, A. F. Izmaylov, J. Bloino, G. Zheng, J. L. Sonnenberg, M. Hada, M. Ehara, K. Toyota, R. Fukuda, J. Hasegawa, M. Ishida, T. Nakajima, Y. Honda, O. Kitao, H. Nakai, T. Vreven, J. A. Montgomery, J. E. Peralta Jr., F. Ogliaro, M. Bearpark, J. J. Heyd, E. Brothers, K. N. Kudin, V. N. Staroverov, T. Keith, R. Kobayashi, J. Normand, K. Raghavachari, A. Rendell, J. C. Burant, S. S. Iyengar, J. Tomasi, M. Cossi, N. Rega, J. M. Millam, M. Klene, J. E. Knox, J. B. Cross, V. Bakken, C. Adamo, J. Jaramillo, R. Gomperts, R. E. Stratmann, O. Yazyev, A. J. Austin, R. Cammi, C. Pomelli, J. W. Ochterski, R. L. Martin, K. Morokuma, V. G. Zakrzewski, G. A. Voth, P. Salvador, J. J. Dannenberg, S. Dapprich, A. D. Daniels, O. Farkas, J. B. Foresman, J. V. Ortiz, J. Cioslowski and D. J. Fox, Gaussian, Inc., Wallingford CT, 2013.
- (11) I. Y. Zhang, J. Wu and X. Xu, *Chem. Comm.*, 2010, **46**, 3057–3070.
- (12) C. J. Cramer and D. G. Truhlar, *Phys. Chem. Chem. Phys.*, 2009, **11**, 10757–10816.
- (13) E. R. Davidson, Ed. *Chem. Rev.*, 2000, **100**, 351–818 (special issue “Computational Transition Metal Chemistry”).
- (14) T. Ziegler and J. Autschbach, *Chem. Rev.*, 2005, **105**, 2695–2722.
- (15) X. Li and M. J. Frisch, *J. Chem. Theory Comput.*, 2006, **2**, 835–839.
- (16) M. Cossi, V. Barone, R. Cammi and J. Tomasi, *Chem. Phys. Lett.*, 1996, **255**, 327–335.
- (17) M. Cossi and V. Barone, *J. Chem. Phys.*, 1998, **109**, 6246–6254.
- (18) M. Cossi, N. Rega, G. Scalmani and V. Barone, *J. Chem. Phys.*, 2001, **114**, 5691–5701.